# MÖSSBAUER EFFECT IN HEMOGLOBIN AND SOME IRON-CONTAINING BIOLOGICAL COMPOUNDS

U. GONSER *and* R. W. GRANT

*From the North American Aviation Science Center, Thousand Oaks, California*

ABSTRACT The Mössbauer effect in $Fe^{57}$ has been used to study the molecules, hemoglobin, $O_2$-hemoglobin, $CO_2$-hemoglobin, and CO-hemoglobin (within red cells) and the molecules, hemin and hematin (in the crystalline state). Quadrupole splittings and isomeric shifts observed in the Mössbauer spectra of these molecules are tabulated. The temperature dependence of the quadrupole splitting and relative recoil-free fraction for hemoglobin with different ligands has been investigated. An estimate of the Debye-Waller factor in $O_2$-hemoglobin at 5°K is 0.83. An asymmetry in the quadrupole splitting observed in hemoglobin is attributed to a directional dependence of the recoil-free fraction which establishes the sign of the electric field gradient in the molecule and indicates that the lowest lying *d* orbital of the Fe atoms is $|xy\rangle$. This asymmetry indicates that the iron atoms in hemoglobin are vibrating farther perpendicular to the heme planes than parallel to them, and, in fact, the ratio of the mean square displacements perpendicular and parallel to the heme planes in hemoglobin is $\approx 5.5$ at 5°K. The temperature dependence of the quadrupole splitting in hemoglobin has been used to estimate a splitting between the lowest lying iron atom *d* orbitals of $\approx 420$ $cm^{-1}$.

## INTRODUCTION

The Mössbauer effect (recoil-free nuclear $\gamma$-ray resonance) has been used to study many interesting problems in physics and chemistry (1 – 4) since its discovery by Mössbauer in 1958 (5, 6). The main difficulty of applying this technique to biophysical studies concerns the extreme dilution of presently available Mössbauer isotopes in most biological compounds. However, this difficulty is an experimental problem which can usually be solved (if necessary with the use of enriched isotopes) and should not prevent the Mössbauer effect from becoming a new and interesting tool for biological research (7).

At present, it appears that only the elements iron and iodine offer reasonable possibilities for Mössbauer experiments of a biological nature. We will restrict our attention to iron in this paper. $Fe^{57}$ has become the most widely used Mössbauer

isotope in physics and chemistry, and it is fortunate that iron is contained in hemoglobin (Hb), myoglobin, cytochrome, peroxidases of plants, catalases of erythrocytes, and other molecules which have interesting biological functions. A number of techniques has been applied to studying the physical and chemical parameters of these iron-containing compounds. Mössbauer effect studies with $Fe^{57}$ should add new information about the nature of these compounds, since the technique allows one to make a non-destructive measurement on an atomic scale and to single out and study only the iron atoms in the sample.

In the present study we will demonstrate the feasibility and applicability of Mössbauer spectroscopy for biophysical studies of compounds containing $Fe^{57}$ and discuss the Mössbauer spectra of hemoglobin and some related porphyrin ring compounds in considerable detail.

## MÖSSBAUER PARAMETERS

The underlying principle of the Mössbauer effect is that a $\gamma$-ray resulting from the transition between excited and ground nuclear states can be emitted in a recoil-free fashion (*i.e.*, the $\gamma$-ray can possess essentially the full nuclear transition energy) if the emitting nucleus is strongly bound in a lattice or molecule. This $\gamma$-ray can excite the reverse nuclear process in an identical nucleus. A Mössbauer spectrum can then be observed by applying a small relative velocity between the emitting and absorbing nuclei to Doppler shift the energy of the recoil-free $\gamma$-ray in and off resonance. There are several extensive review articles which discuss the origin and interpretation of parameters measured by Mössbauer spectroscopy (8 – 11). Since comparatively few Mössbauer studies of a biological nature have been published, in this section we present a highly condensed formulation of these parameters which is useful in discussing our experimental results.

*Recoil-Free Fraction.* The intensity of a Mössbauer absorption line is determined by the recoil-free fraction, $f$, which can be expressed in a general form as

$$f = \exp - \langle x^2 \rangle K^2 \tag{1}$$

where $\langle x^2 \rangle$ is the mean square displacement component of the resonating atom in the $\gamma$-ray emission direction, $K$ is the wave number $(2\pi/\lambda)$, and $\lambda$ is the $\gamma$-ray wavelength.

If the Debye model is used to represent the vibrational frequency spectrum of the solid, the Debye-Waller factor (which was developed in the theory of the temperature dependent x-ray scattering) gives the fraction of recoil-free processes.

The appropriate form of this factor is, (see reference 12)

$$f = \exp\left\{-\frac{3}{2}\frac{E_R}{k\theta_D}\left[1 + 4\left(\frac{T}{\theta_D}\right)^2 \int_0^{\theta_D/T} \frac{x}{e^x - 1}\,dx\right]\right\} \tag{2}$$

where $E_R$ is the free atom recoil energy, $k$ is the Boltzmann constant, $\theta_D$ is the effec-

tive Debye temperature of the Mössbauer atom in its environment, and $T$ is the absolute temperature of the solid. The free atom recoil energy is just

$$E_R = \frac{E_\gamma^2}{2mc^2} \tag{3}$$

where $E_\gamma$ is the $\gamma$-ray energy, $m$, the mass of the recoiling nucleus, and $c$, the velocity of light.

In the low temperature limit equation (2) reduces to

$$f = \exp\left\{-\frac{3}{2}\frac{E_R}{k\theta_D}\left[1 + \frac{2}{3}\left(\frac{\pi T}{\theta_D}\right)^2\right]\right\} \qquad T \ll \theta_D \tag{4}$$

which is accurate to a few per cent for $T \lesssim 0.3\ \theta_D$. For higher temperatures, one must evaluate equation (2) which has been done by Muir (13).

In more complicated solids or molecules (such as the ones studied in the present investigation), the simple Debye model which contains only acoustical vibrational modes may not be sufficient and one also must consider the effect of optical modes. An optical vibrational branch in a solid can be characterized by a single vibrational frequency and the relevant expression for the recoil-free fraction becomes, (see reference 11)

$$f = \exp\left\{-\frac{E_R}{k\theta_E}\coth\frac{\theta_E}{2T}\right\} \tag{5}$$

where the effective Einstein temperature, $\theta_E$, is related to the characteristic oscillator frequency, $\omega_E$, by

$$\theta_E = \frac{\hbar\omega_E}{k} \tag{6}$$

and $\hbar$ is Planck's constant, $h$, divided by $2\pi$. Thus, in general, to interpret a recoil-free fraction measured in a complicated solid, one must consider both the acoustical and optical branches of the phonon spectrum.

*Hyperfine Interactions.* The nominal energy and splitting of a nuclear state can be described in terms of a spin Hamiltonian

$$\mathcal{H} = E + GI_z + P\left[I_z^2 - \frac{I}{3}(I+1) + \frac{\eta}{3}(I_x^2 - I_y^2)\right] \tag{7}$$

where the first term represents an electric monopole interaction (responsible for the isomeric shift), the second term represents the magnetic dipole interaction, and the third term represents an electric quadrupole interaction (we have assumed that the magnetic field is parallel to the $z$ axis of the electric field gradient tensor, which has been transformed to principle axes, and interactions of higher order than quadrupole have been neglected). $I_x$, $I_y$, and $I_z$ are the projections of the nuclear spin, $I$, along the $x$, $y$, and $z$ directions, and $\eta$ is an asymmetry parameter which contains the com-

ponents of the electric field gradient tensor $\eta = (V_{xx} - V_{yy})/V_{zz}$. The hyperfine structure constant, $G$, and the quadrupole coupling constant, $P$, are defined as

$$G = -\frac{\mu}{I} H$$
$$P = \frac{3e^2qQ}{4I(2I - 1)} \tag{8}$$

where $\mu$ is the nuclear magnetic moment, $H$, is the effective magnetic field at the nucleus, $e$, is the charge of the electron, $q = V_{zz}/e$, and $Q$ is the nuclear quadrupole moment. To determine the position of absorption lines, one must calculate the energy levels of the ground state and excited state in both source and absorber using the appropriate terms in equation (7). The transitions between these energy levels will then be given by the selection rules appropriate for the multipolarity of the $\gamma$-ray.

The isomeric shift, $\delta$, (in the non-relativistic approximation) can be expressed as, see reference (14)

$$\delta = C \frac{\delta R}{R} [\psi_A^2(0) - \psi_S^2(0)] \tag{9}$$

where $C$ contains parameters which are constant for a given isotope, $R$ is the nuclear radius, $\delta R = R_{\text{excited}} - R_{\text{ground}}$, and the term in brackets represents the difference in the total electron density evaluated at the nucleus, $\psi^2(0)$, between source and absorber atoms. This term contains information that can be interpreted in terms of chemical bonding and is the reason that $\delta$ is also called the chemical shift.

## $Fe^{57}$ IN PORPHYRIN RING COMPOUNDS

The compounds which have been studied in the present investigation all have in common that the central iron-containing configuration is a porphyrin ring. In Fig. 1 we show, as an example of this structure, the configuration around the Fe atoms in hemoglobin. The iron atom is located at the center of the porphyrin ring formed by four nitrogen atoms, the globin molecule occupies the 5 position, and the 6 position

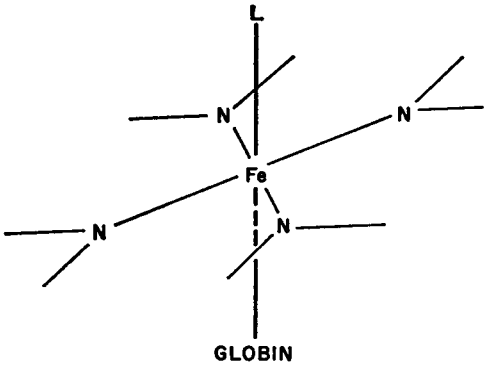


FIGURE 1 Structure immediately surrounding the iron atoms in hemoglobin.

is usually occupied by a ligand, $L$. The ease with which the ligand can be exchanged and the electronic transitions ($Fe^{++} \rightleftarrows Fe^{+++}$; high spin $\rightleftarrows$ low spin) are some of the interesting functions of the porphyrin ring compounds (15) which can be investigated *via* the Mössbauer effect.

The Mössbauer transition in $Fe^{57}$ involves a 14.4 kev $\gamma$-ray which converts the $I = 3/2$ excited state to the $I = 1/2$ ground state ($I$ is the nuclear spin). Although the exact details of the bonding to the globin molecule and to various ligands are still somewhat in dispute, to a first approximation the iron atom in the porphyrin ring is located in an axially symmetric configuration (probably a fourfold rotational axis) at least with respect to its nearest neighbors. It is well established in some iron-containing porphyrin ring compounds that the iron atom is slightly displaced out of the porphyrin ring plane (16). However, as long as the bond lengths between the iron atom and the four nitrogen atoms of the ring remain equal, the iron atom will still possess axial symmetry with respect to its nearest neighbors. The asymmetry parameter in equation (7) will, therefore, be small for Fe in porphyrin ring compounds, and we will assume it is zero.

In our experiments we have used biological compounds as absorbers in conjunction with a single line source. All hyperfine splittings which we observe in these compounds can be attributed to a quadrupole interaction in the $I = 3/2$ excited state of the absorber (except possibly in hemin and hematin, see Discussion section). The ground state of $Fe^{57}$ has $I = 1/2$ which precludes a quadrupole interaction. With the above assumption ($\eta = 0$), we can now use equation (7) to obtain the approximate expression for the quadrupole splitting (peak separation), $\Delta E_Q$, of $Fe^{57}$ in porphyrin ring compounds

$$\Delta E_Q = 1/2e^2qQ \tag{10}$$

where $q$ can be treated as a scaler (because $\eta = 0$), and $Q = +0.29$ barn (17) is the nuclear quadrupole moment of the $I = 3/2$ excited state in $Fe^{57}$. The multipolarity of the 14.4 kev $\gamma$-ray is mainly M1 which has the selection rules $\Delta I_z = 0, \pm 1$.

## EXPERIMENTAL TECHNIQUES AND RESULTS

*Source.* Our source consisted of approximately 10 mc of $Co^{57}$ diffused into Pt[1] and kept at room temperature during the measurements. Values of the isomeric shift are quoted with respect to this source.

*Absorbers.* The hemoglobin absorbers, with one exception, were prepared from human blood (taken from a vein) which was washed several times with saline solution. The ligand in the hemoglobin molecule was varied by bubbling an appropriate gas (CO, $O_2$, $N_2$, $CO_2$) through the blood and preventing exposure to air thereafter. Before placing the blood into the absorber holder, the red cells were concentrated by centrifuging.[2] The

[1] This source was obtained commercially from the Nuclear Science and Engineering Corporation, Pittsburgh, Pennsylvania.

[2] In a preliminary study (18) the red cells were allowed to sediment. However, it was experimentally determined that centrifuging produced no change in the Mössbauer spectra and

absorber was then mounted in a cryostat and cooled to 80°K before evacuating the cryostat and adjusting the absorber temperature to the desired value.

One hemoglobin absorber was prepared from rat blood which was isotopically enriched with $Fe^{57}$ so that about 3.5 per cent of the Fe atoms were $Fe^{57}$ (natural abundance is 2.2 atomic per cent). The enrichment was accomplished by injecting a rat with a 1 per cent solution of phenylhydrazine hydrochloride to produce hemolysis. Concommitantly, the rat was injected with an $Fe^{57}$ chloride solution. The new red blood cells were able to incorporate some of the $Fe^{57}$ and the enriched blood was drawn from the rat about four weeks after the injections.[3] The hemin and hematin absorbers were obtained commercially[4] as fine powders and were studied in the crystalline state.

*Mössbauer Apparatus.* The basic components of our mechanical drive system are shown schematically in Fig. 2. A "barrel" cam drove the source in both forward and reverse directions at constant velocity. By adjusting the ball-disc integrator, the velocity could be varied between 0 and 15 mm/second. In all experiments the absorber was stationary. The detector was a 1 mm thick NaI(Tl) scintillation crystal coupled to a standard photomultiplier tube. A conventional amplifier and single channel analyzer were used to select pulses produced by the 14.4 kev $\gamma$-ray, and these pulses were stored in one of two scalers depending on whether the source was moving with positive or negative velocity (positive velocity is defined as source moving toward absorber).

Photoelectric gating was used to route pulses alternately between the two scalers and also to block the storage of pulses while the source was reversing direction. The absorber temperature was measured by a Cu–(Au-2.1 at. per cent Co) thermocouple or a gallium-doped germanium resistance thermometer. The outer windows of the cryostat were 0.25 mm Be and the radiation shield windows were 0.006 mm Al foil.

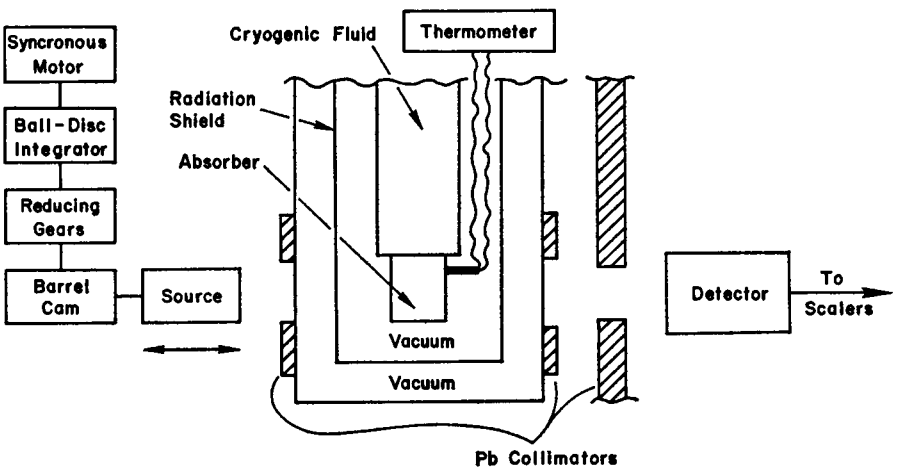


FIGURE 2 Schematic diagram of the Mössbauer spectrometer.

since this process significantly increases the concentration of hemoglobin (and, therefore, the signal to noise ratio), most absorbers in the present study were centrifuged.

[3] We are indebted to Dr. J. Kregzde for preparing this absorber.

[4] These absorbers were obtained commercially from the California Corporation for Biochemical Research, Los Angeles, California.

*Low Temperature Results.* In Fig. 3 we show several Mössbauer spectra taken at 5°K. The absorbers used to obtain these spectra were: (*a*) rat red cells, isotopically enriched with $Fe^{57}$ as described above. This absorber was prepared by sedimentation (all other hemoglobin absorbers were centrifuged) which is the reason that the maximum absorption (dip) of the spectrum does not appear to be enhanced over the following spectra. To observe this enhancement, one must compare two similarly prepared absorbers as was done in reference (18). (*b*) human red cells, 5 minutes exposure to $0_2$ gas; (*c*) human red cells, 15 minute exposure to $0_2$ gas; (*d*) human red cells, 15 minute exposure to $CO_2$ gas; (*e*) human red

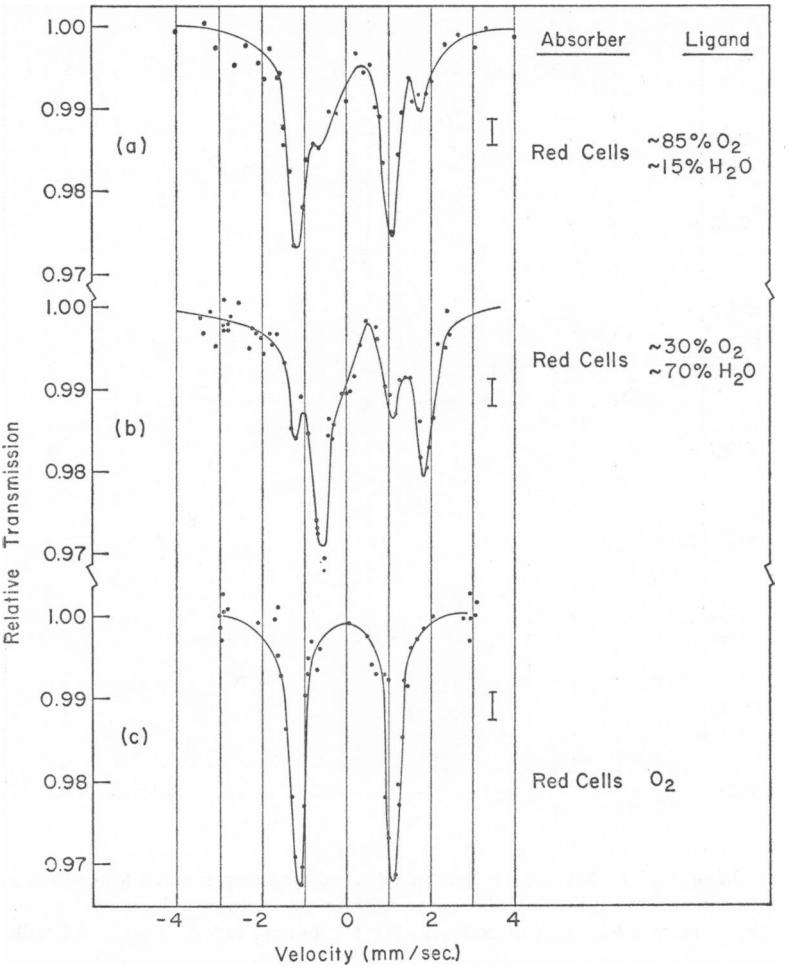


FIGURE 3*a*, *b*, and *c* Mössbauer spectra obtained by using a room temperature $Co^{57}$ in Pt source and the following absorbers at 5°K: (*a*) veinous rat red cells isotopically enriched with $Fe^{57}$; (*b*) human red cells after a 5 minute exposure to $O_2$ gas; (*c*) human red cells saturated with $O_2$ gas.

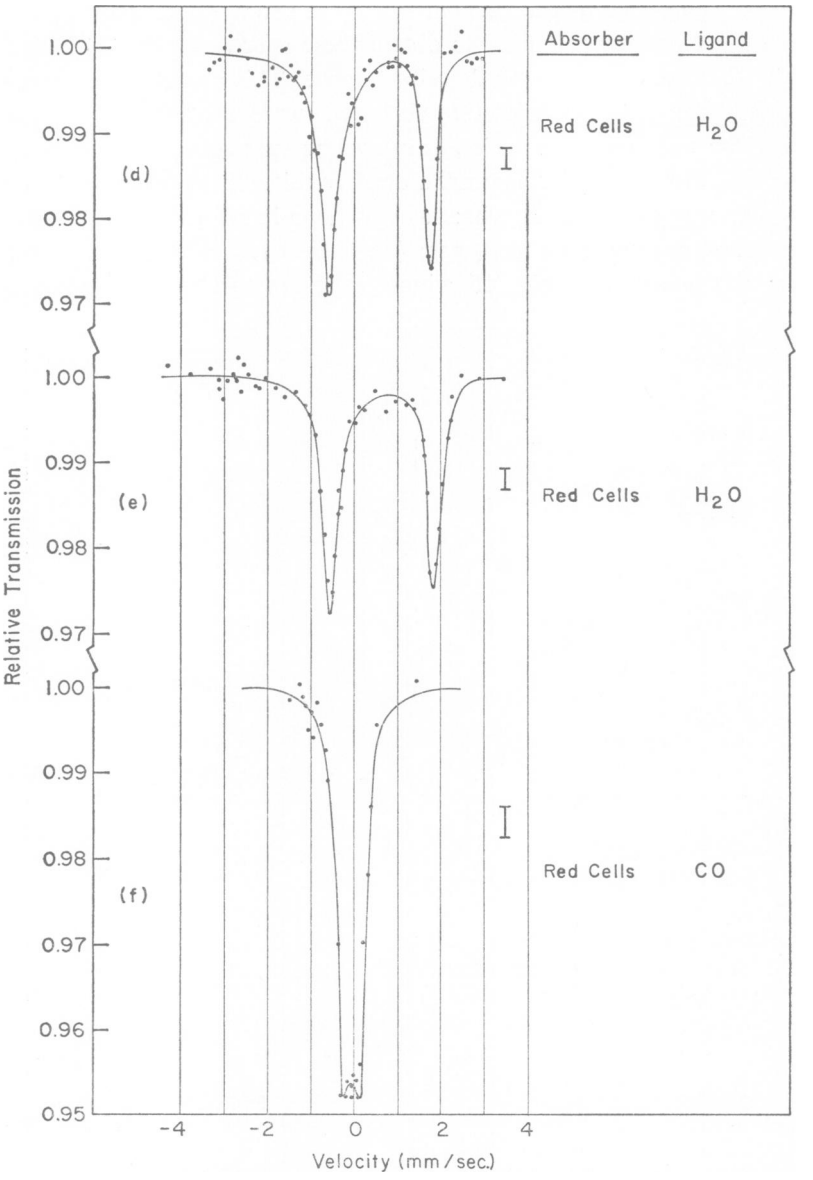


FIGURE 3*d*, *e*, and *f* Mössbauer spectra obtained by using a room temperature $Co^{57}$ in Pt source and the following absorbers at 5°K: (*d*) human red cells saturated with $CO_2$; (*e*) human red cells saturated with $N_2$; (*f*) human red cells saturated with CO.

cells, 15 minute exposure to $N_2$ gas; (*f*) human red cells, 15 minute exposure to CO gas; (*g*) crystalline hemin; (*h*) crystalline hematin.

In Table I the data on isomeric shift and quadrupole splitting are summarized.

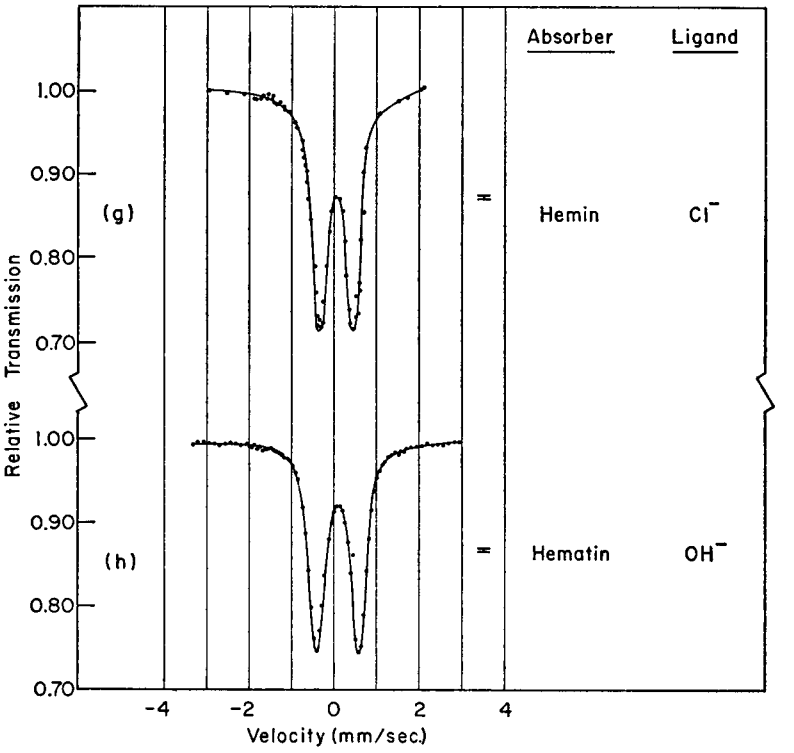


FIGURE 3*g* and *h* Mössbauer spectra obtained by using a room temperature $Co^{57}$ in Pt source and the following absorbers at 5°K: (*g*) crystalline hemin; (*h*) crystalline hematin.

TABLE I

QUADRUPOLE SPLITTINGS AND ISOMERIC SHIFTS OBSERVED IN SEVERAL COMPOUNDS AT 5°K

| Absorber | Ligand | Quadrupole splitting (peak separation) | Isomeric shift* |
|---|---|---|---|
| | | *mm/sec.* | *mm/sec.* |
| Red cells | $O_2$ | 2.25 ± 0.05 | −0.08 ± 0.05 |
| | $H_2O$ | 2.4 ± 0.1 | +0.59 ± 0.05 |
| Red cells $O_2$-atmosphere | $O_2$ | 2.25 ± 0.03 | −0.08 ± 0.02 |
| Red cells $CO_2$-atmosphere | $H_2O$ | 2.35 ± 0.05 | +0.58 ± 0.03 |
| Red cells $N_2$-atmosphere | $H_2O$ | 2.36 ± 0.05 | +0.59 ± 0.03 |
| Red cells CO-atmosphere | CO | 0.34 ± 0.05 | −0.07 ± 0.03 |
| Hemin (crystalline) | $Cl^-$ | 0.78 ± 0.03 | +0.09 ± 0.02 |
| Hematin (crystalline) | $(OH)^-$ | 0.98 ± 0.03 | +0.08 ± 0.02 |

*Relative to the $Co^{57}$ in Pt source at room temperature.

The fact that spectra 3*d* and 3*e* are identical to within experimental error is confirmation that the $CO_2$ molecule in $CO_2$-Hb is not bound as a ligand in the 6 position but is attached to some other part of the molecule.

*Temperature Dependence of Dip.* In Fig. 4 the minimum relative transmission (maximum dip) of the Mössbauer spectra is plotted as a function of temperature for 3 human blood samples which were first exposed to $O_2$, CO, and $N_2$

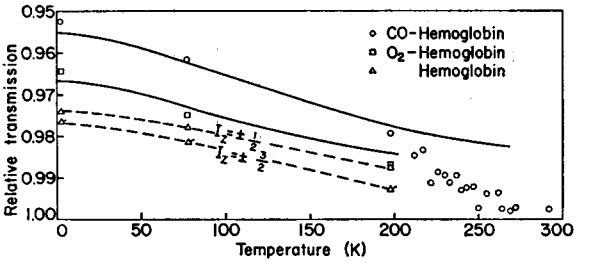


FIGURE 4 Minimum relative transmission *vs.* temperature for absorbers of human red cells which were saturated with CO, $O_2$, and $N_2$ gases.

gases. The maximum absorption is largest in CO-hemoglobin owing to the partially overlapping lines. A measurement on CO-hemoglobin was performed at room temperature and appeared to give a small resonance even at this temperature. However, more refined measurements (which probably include enrichment with $Fe^{57}$) are needed to determine if an effect in liquid blood is measurable at room temperature. The spectrum of deoxygenated blood (hemoglobin) has two lines with different intensities. These lines are designated $I_z = \pm 3/2$ and $I_z = \pm 1/2$ because they represent (as will be shown in the Discussion section) $\gamma$-ray transitions to these excited nuclear states.

*Thickness Dependence of Mössbauer Spectra.* A careful investigation of the $O_2$-hemoglobin Mössbauer spectrum was made as a function of absorber thickness. A blood sample was oxygenated and centrifuged. The iron concentration of this sample was determined chemically[5] as 1.2 mg Fe/cm.[3] Since the natural abundance of $Fe^{57}$ is 2.2 per cent, this gives an $Fe^{57}$ concentration of about 0.026 mg $Fe^{57}$/cm.[3] In Fig. 5 the average dip of the two absorption lines and the total absorption area of the $O_2$-hemoglobin spectrum is plotted as a function of thickness (in both mg Fe/cm$^2$ and the actual physical absorber thickness in centimeters). The curves in Fig. 5 should help one estimate both the $Fe^{57}$ concentrations necessary to observe useable Mössbauer effects in biological compounds and absorber thicknesses necessary to maximize the resonance effect (the solid lines in Fig. 5 are discussed in the Discussion section). In an actual experiment, one does not usually want to maximize the resonance effect (unless a very strong source is available) because at

[5] We are indebted to Dr. E. P. Parry for this analysis.

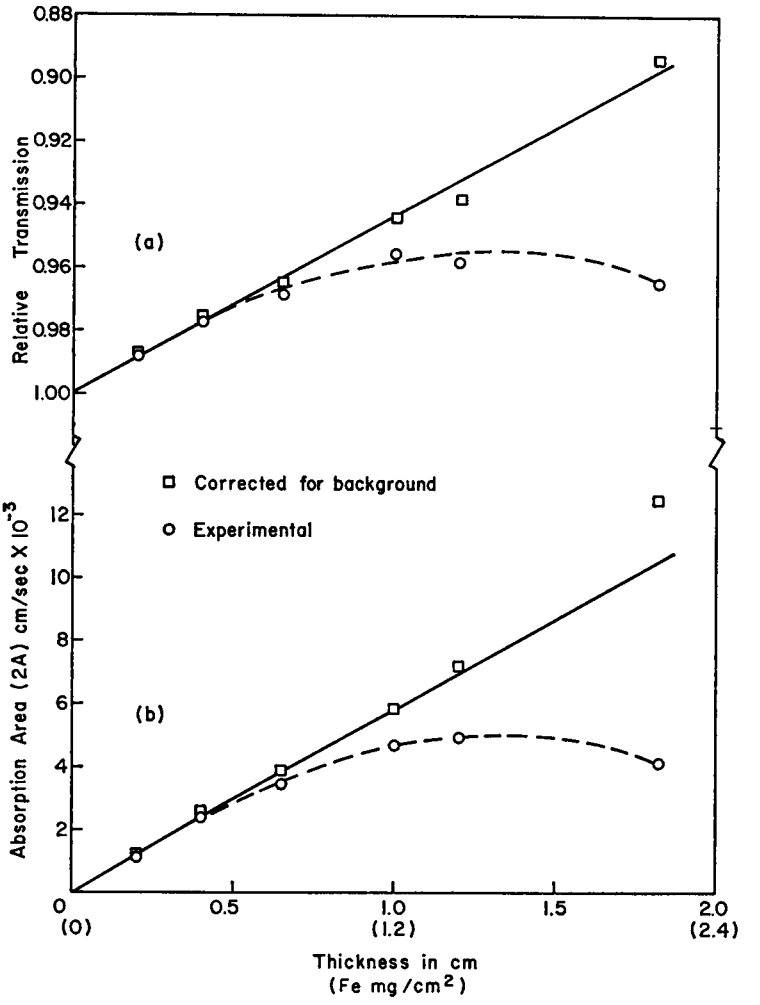


FIGURE 5 (*a*) Average minimum relative transmission of the two $O_2$-hemoglobin absorption lines, and (*b*) total absorption area under the $O_2$-hemoglobin spectrum *vs.* the absorber thickness in both cm and mg Fe/cm².

the maximum resonance photoelectric absorption is so large that long counting times are needed to obtain reasonable statistics. For red cells the resonance absorption is a maximum at about 1.4 cm and with thicker absorbers, gradually decreases to zero because photoelectric absorption becomes extremely large (and the 14.4 kev $\gamma$-ray to background ratio becomes very small).

In Fig. 6 we have plotted the background factor, $B$, which is defined as

$$B = \frac{A_B}{A_\gamma + A_B} \tag{11}$$

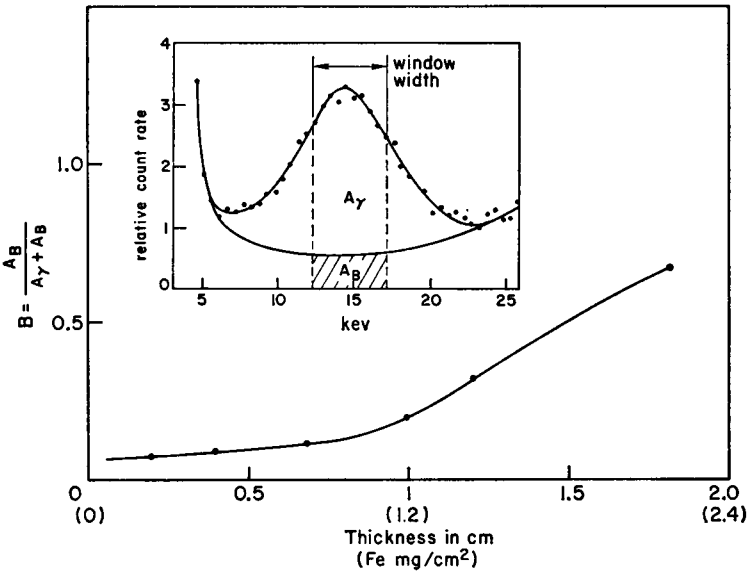


FIGURE 6 Background factor *vs.* absorber thickness for $O_2$-hemoglobin absorbers. The insert shows a typical pulse height spectrum taken through a 1 cm thick $O_2$-hemoglobin absorber. The window width of the single channel analyzer, which defines $A_B$ and $A_\gamma$, is also indicated in the insert.

where $A_\gamma$ and $A_B$ are the fraction of pulses stored in the scalers which are due to 14.4 kev $\gamma$-rays and background, respectively. The insert in Fig. 6 shows a typical $\gamma$-ray pulse height spectrum of the 14.4 kev $Fe^{57}$ $\gamma$-ray transmitted through a red cell sample 1 cm thick ($A_\gamma$ was determined by subtracting a Gaussian curve from the pulse height spectrum until a smooth background remained and noting the window width of the single channel analyzer). Fig. 6, of course, is only appropriate for our particular source, absorbers, detector, geometry, etc.; however, since in most experiments these conditions will probably not change too severely, this figure can be used to estimate roughly how $B$ varies with thickness. With our experimental parameters (10 mc source, source to detector distance = 12 cm), the "optimum" experimental absorber thickness was 0.8 to 1.0 cm.

The line widths of the $O_2$-hemoglobin resonance lines were also investigated as a function of absorber thickness by computer least squares fitting the experimental spectra with two superimposed Lorentz curves. (The line width refers to the full width of the resonance line at half maximum.) The experimental line width, $\Gamma_{exp}$, was found to be essentially thickness-independent with an average value of 0.34 mm/second. In general, the apparent line width, $\Gamma_a$, is a function of the effective absorber thickness, $T_A$, (19)

$$T_A = f_A \sigma_0 n_A t_A a_A \tag{12}$$

where $f_A$ is the recoil-free fraction in the absorber, $n_A$, the number of Fe atoms per $cm^3$ in the absorber, $t_A$, the physical thickness of the absorber in centimeters and $a_A$ is the isotopic abundance of $Fe^{57}$. $\sigma_0$ is the Mössbauer absorption cross-section which is given by, (see reference 9)

$$\sigma_0 = \frac{\lambda^2(1 + 2I_{ex})}{2\pi(1 + 2I_g)(1 + \alpha)} \tag{13}$$

where $I_{ex}$ and $I_g$ are the nuclear spins of the excited and ground states, respectively, and $\alpha$ is the internal conversion coefficient.[6] Assuming the natural line width, $\Gamma$, ($\Gamma = \hbar/\tau$ where $\tau$ is the mean lifetime of the excited nuclear state) in both the emission and absorption lines and for values of $T_A \lesssim 5$, (see reference 9)

$$\frac{\Gamma_a}{\Gamma} = 2 + 0.27T_A. \tag{14}$$

The iron concentration of the thickest absorber used in Fig. 5 was 2.2 mg/$cm^2$ which corresponds to $T_A' = 0.51$ using $f_A = 0.83$ and taking into account the removal of degeneracy by the quadrupole interaction (see Discussion section). According to equation (14) this absorber thickness would produce a broadening in the resonance line of less than 0.02 mm/second. The observed thickness independence of $\Gamma_{exp}$ is, therefore, not surprising since 0.02 mm/second is within the accuracy to which $\Gamma_{exp}$ could be experimentally determined. The experimental line width in $O_2$-hemoglobin is about 1.8 times the theoretically expected line width, $2\Gamma$. This is quite narrow even in comparison with many crystalline inorganic iron compounds (4). Neglecting instrumental line broadening and assuming the emission line width of the source, $\Gamma_s = \Gamma$, leads to an upper limit of the absorption line width, $\Gamma_A$, of $\Gamma_A \simeq 2.4\ \Gamma$. The actual $\Gamma_A$ is probably somewhat smaller than this value which implies that the distributions of electric field gradients and electronic densities at the Fe nuclei in $O_2$-Hb are fairly small and that the structure of $O_2$-hemoglobin at least in the vicinity of the Fe atoms is rather unique.

*Temperature Dependence of the Electric Field Gradient.* The temperature dependence of the quadrupole splitting in hemoglobin, $O_2$-hemoglobin, and CO-hemoglobin is shown in Fig. 7. The small electric field gradient (EFG) in CO-hemoglobin permits only a partial resolution of the two absorption peaks which was missed in our preliminary study (18). Because no change in the over-all width of the absorption spectrum was observed, the electric field gradient in CO-hemoglobin appears to be essentially temperature independent. In both hemoglobin and $O_2$-hemoglobin, there is about a 12 per cent decrease in the quadrupole splitting between 5° and 195°K.

---

[6] We have used $\alpha = 9.0 \pm 0.4$ for the 14.4 kev $\gamma$-ray in $Fe^{57}$ which is the recently determined value of R. H. Nussbaum and R. M. Housley (20).

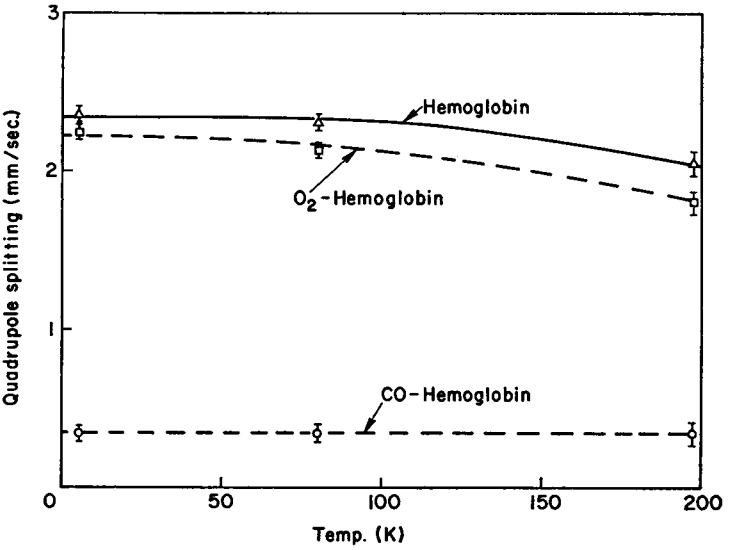


FIGURE 7 Quadrupole splitting (peak separation) *vs.* temperature in hemoglobin, $O_2$-hemoglobin, and CO-hemoglobin.

## DISCUSSION OF RESULTS

*Estimate of f in $O_2$-Hb.* In a typical Mössbauer experiment, one measures the difference between resonant and non-resonant counting rates which we will designate $(C_R)_{exp}$ and $(C_N)_{exp}$, respectively. The experimental counting rates include the background counting rate, $B_K$, so that the "true" relative transmission is

$$\frac{C_R}{C_N} = \frac{(C_R)_{exp} - B_K}{(C_N)_{exp} - B_K} \tag{15}$$

If we now define the background factor, $B$, as in equation (11), $B_K = B(C_N)_{exp}$ and equation (15) becomes

$$\frac{C_R}{C_N} = \frac{(C_R/C_N)_{exp} - B}{1 - B} \tag{16}$$

We will consider two methods of evaluating $f$ for $O_2$-Hb: the dip and the area method. Assuming $\Gamma_s = \Gamma$, the maximum dip can be expressed as

$$\text{dip}_{max} = 1 - \left(\frac{C_R}{C_N}\right)_{max} = f_s\left[1 - e^{-T_A'/2} J_0\left(i\,\frac{T_A'}{2}\right)\right] \tag{17}$$

where $f_s$ is the recoil-free fraction in the source,[7] $T_A'$ is a corrected value of $T_A$ which takes into account the degeneracy of the nuclear states (*i.e.* $T_A' = T_A$ for a

[7] A precise determination of $f_s = 0.72 \pm 0.02$ for our $Co^{57}$ in Pt source at room temperature was made by A. H. Muir, Jr. using the black absorber method (unpublished data).

single line absorption spectrum, but for $O_2$-Hb where a well resolved quadrupole splitting is present, $T_A' = 0.5\ T_A$), and $J_0$ is the Bessel function of zero order. One can then determine $f_A$ for $O_2$-Hb by correcting the data of Fig. 5*a* with equation (16) and solving equation (17) for $f_A$. The value of $f_A$ determined in this way is 0.49. This value should be considered only as a lower limit since one makes the implicit assumption in equation (17) that the absorption line width is $2\Gamma$ which is not experimentally justified as pointed out in Experimental Techniques and Results section. Perhaps a better estimate for $f_A$ could be obtained in this case by multiplying the value of $f_A$, as determined from equation (17), by $\Gamma_{exp}/2\Gamma$ to correct roughly for the observed line broadening. This correction leads to a value $f_A = 0.88$ in good agreement with the value determined below.

The area analysis method is discussed in detail by Shirley, Kaplan, and Axel (21). For $t \lesssim 2$ the absorption area (in cm/second), $A$, of a single line spectrum can be approximately expressed as

$$A = \frac{\pi}{2}\frac{c}{E_\gamma} T_A \Gamma f_a (1 - 0.24t + 0.04t^2) = \frac{\pi}{2}\frac{c}{E_\gamma}\Gamma_{exp}\left[1 - \left(\frac{C_R}{C_N}\right)_{max}\right] \tag{18}$$

where $E_\gamma$, $\Gamma$ and $\Gamma_{exp}$ are measured in the same units and $t = T_A\Gamma/\Gamma_A$. As in equation (17), $T_A$ in equation (18) must be replaced by $T_A'(= 0.5\ T_A)$ to analyze the quadrupole split absorption spectrum of $O_2$-Hb. In this case $A$ represents the absorption area under each line and the total absorption area is $2A$. The experimental absorption area, $2A_{exp}$, shown in Fig. 5*b* must be corrected for background in the same manner as the dip is corrected and in this case the appropriate correction becomes

$$2A = \frac{(2A)_{exp}}{1 - B} \tag{19}$$

The corrected data are shown as squares in this figure and the solid line through the corrected data is calculated from equation (18) for

$$f_{a,-Hb} = 0.83 \tag{20}$$

and represents the best fit of this data. In this calculation we have somewhat arbitrarily used $\Gamma_A = 0.24$ mm/second which assumes $\Gamma_S = \Gamma$ and no instrumental broadening. These assumptions are reasonable since experimental line widths approaching $2\Gamma$ have been obtained by using the same source and other absorbers; also, it is fortunate that $f_A$, as determined by the area method analysis, is not strongly dependent on the choice of $\Gamma_A$. One can calculate the dip $[1 - (C_R/C_N)_{max}]$ from equation (18)

$$\text{dip} = \frac{T_A \Gamma f_a (1 - 0.24t + 0.04t^2)}{\Gamma_{exp}} \tag{21}$$

and this curve is shown as the solid line in Fig. 5*a* (again, $T_A$ in equation (21) must be replaced by $T_A'$). The area method, which is relatively insensitive to the absorption

line width, should give a considerably better estimate of $f_{O_2-Hb}$ than the dip method. Experimental errors and uncertainties in $\alpha$, $n_A$, $t_A$, and $f_s$ make it difficult to estimate meaningful error limits for $f_{O_2-Hb}$; however, we feel the error in equation (20) is on the order of $\pm 10$ per cent. The accuracy of the data in Fig. 5 for the 1.8 cm thick sample is very poor due to the large background, and therefore, this point has been ignored in the above $f$ analysis.

*Recoil-Free Fraction and Mean Square Displacement.* For samples with small $T_A$, such as those in the present study, the relative absorption (corrected for background) is nearly proportional to the recoil-free fraction, $f_A$. Therefore, the temperature dependence of the relative absorption as shown in Fig. 4 is essentially the temperature dependence of $f_A$. As calculated above, the recoil-free fraction in $O_2$-Hb at 5°K is $f_A \approx 0.83$. The proportionality of relative absorption and $f$ applies to each absorber individually; however, Fig. 4 also reflects, to a first approximation, the relative $f_A$ of the three absorbers because the thickness and iron concentration of the absorbers in all cases were similar. Of course, in such a comparison only one component of the unresolved CO-hemoglobin spectrum should be considered; whereas, in Fig. 4, the maximum dip of the partially overlapping lines is plotted. The recoil-free fraction for $O_2$-hemoglobin and CO-hemoglobin is the same to within our experimental accuracy. A thickness study similar to that in $O_2$-Hb was not performed for CO-Hb and Hb. The experimental points for $O_2$-Hb and CO-Hb in Fig. 4 can be fitted with an $f_A$ derived from a Debye frequency spectrum (equation 2) with $\theta_D \approx 180$°K and these theoretical curves are shown as solid lines. If the vibrational spectrum were characterized by the Einstein model, $f_{O_2-Hb} = 0.83$ would correspond to a $\theta_E \simeq 120$°K. With the aid of equation (5), it can be shown that the Einstein model does not fit the data as well as the Debye model. The determination of $f_{O_2-Hb}$ may be used to evaluate the mean square displacement of the Fe atoms in $O_2$-Hb and CO-Hb from equation (1) as $\langle x^2 \rangle_{5°K} \approx 0.35 \times 10^{-18}$ cm$^2$.

In the $O_2$-Hb spectrum the quadrupole split lines are observed to have the same intensity, and therefore, $f$ should be isotropic, while the quadrupole split lines of the Hb spectrum are considerably asymmetric (Fig. 3*d* and *e*). An asymmetry in quadrupole split lines can be observed when $f$ is isotropic if there is a preferential orientation of molecules in the absorber (8). However, in our case where the Hb is still mainly within the red cells, this possibility seems extremely unlikely. Since we have observed no asymmetry with either CO-Hb or $O_2$-Hb samples prepared in the same manner and have observed the same asymmetry in different Hb samples, the obvious conclusion is that $f$ is a function of direction in Hb, and therefore, the Debye model (which is isotropic in nature) cannot be a good representation of the vibrational spectrum of this molecule. The Hb molecule has essentially the same central structure around the Fe atoms as in $O_2$-Hb with the exception that the strongly bound $O_2$ molecule has been removed. One can assume that the elimination of this bond allows the Fe atoms to vibrate farther out of plane than in plane which makes $f$ smaller perpendicular to the heme plane.

The origin of an asymmetry in quadrupole split lines as a result of a directionally dependent $f$ has been discussed in connection with tin organic compounds (22). For a random distribution of molecules, an expression has been worked out for the ratio, $U$, of the two line intensities (using a harmonic approximation) and can be expressed as

$$U = \frac{J_{3/2}}{J_{1/2}} = \frac{\int_0^1 (1 + u^2) \exp(-\epsilon u^2)\, du}{\int_0^1 (5/3 - u^2) \exp(-\epsilon u^2)\, du} \qquad (21)$$

$$\epsilon = K^2(\langle z^2 \rangle - \langle x^2 \rangle)$$

where $\langle z^2 \rangle$ and $\langle x^2 \rangle$ are the mean square displacements parallel and perpendicular to the $z$ axis of the electric field gradient tensor and $J_{3/2}$ and $J_{1/2}$ are the intensities of the $\gamma$-ray transitions to the $\pm 3/2$ and $\pm 1/2$ excited nuclear states. $U$ as a function of $\varepsilon$ has been evaluated numerically (23) and from our data we can derive that $[\langle z^2 \rangle - \langle x^2 \rangle]_{5°K} = 1.6 \times 10^{-18}$ cm$^2$ for the Fe atom in the Hb molecule. If we assume that $\langle x^2 \rangle$ in both Hb and $O_2$-Hb are about equal, $\langle z^2 \rangle_{5°K}$ in Hb is about $1.95 \times 10^{-18}$ cm$^2$ and the recoil-free fractions parallel and perpendicular to the EFG in Hb are $f_{//}$ (5°K) $\approx 0.35$ and $f_{\perp}$ (5°K) $\approx 0.83$, respectively.

As shown in Fig. 4 the Debye model (equation 2) can be used to give a reasonable fit to the experimentally observed temperature dependence of $f$ in $O_2$-Hb and CO-Hb. Since the basic structure of the Hb molecule is probably not significantly changed by removing the $O_2$ molecule, it is, therefore, tempting to associate the decrease in the recoil-free fraction along the EFG direction in Hb with a single vibrational mode superimposed on the vibrational spectrum of $O_2$-Hb and directed perpendicular to the heme plane. A $\theta_E \approx 27$°K ($\omega_E \approx 6 \times 10^{11}$ cycles/second) would account for the low temperature asymmetry of the quadrupole split lines in Hb.

Although most molecular vibrations normally give frequencies in the infrared region ($10^{12} - 10^{14}$ cycles/second), these frequencies are strongly dependent on potential barriers (*e.g.*, the inversion frequency of the $NH_3$ molecule is $2.4 \times 10^{10}$ cycles/second) (24). As noted previously, the equilibrium position of the Fe atom in Hb is slightly displaced out of the heme plane, and it seems possible that a vibration perpendicular to this plane would be slightly hindered. Thus a frequency of $6 \times 10^{11}$ cycles/second may not be unreasonable. A careful measurement of the Hb Mössbauer spectrum as a function of temperature (probably using Hb isotopically enriched with $Fe^{57}$) could determine if one is justified in associating a single vibrational mode with the anisotropic $f$ in Hb and might warrant a search for this mode by more conventional spectroscopic techniques.

*Hyperfine Interactions.* Several hundred iron compounds have been studied by Mössbauer spectroscopy (4) and the spectra are mainly interpreted in terms of isomeric shifts, quadrupole splittings, and in some cases, magnetic hyperfine

interactions. Attempts to evaluate these data in terms of chemical bonding, crystal field theory, or ligand field theory are still rather primitive, probably owing to the rather complicated electronic configuration of iron ($\delta$ in iron compounds will certainly depend on the ionic state, hybridization, polarization, etc.).

Attempts have been made by various investigators to interpret the isomeric shifts of iron compounds qualitatively considering the shielding of $\Psi^2(0)$ by $p$ and $d$ electrons (25) and in terms of partial isomeric shifts due to various ligands (26); however, at present no theory is available which allows a completely satisfactory derivation of chemical parameters. This situation may be somewhat simpler in other Mössbauer isotopes where, for example, in $Au^{197}$ a correlation of the isomeric shift and electronegativity has been established (27).

A few very useful qualitative observations regarding the isomeric shifts in iron compounds have been made, namely, that $\delta$ for iron in different ionic ($Fe^{2+}$ and $Fe^{3+}$) and covalent ($Fe^{II}$, $Fe^{III}$, and $Fe^{VI}$) states fall within certain ranges (28). Another interesting empirical correlation between the isomeric shift and the quadrupole splitting has been reported for a series of covalent compounds by Collins and Pettit (29), and for both high and low spin iron compounds by Remy and Pollak (30). Since Hb ($Fe^{2+}$), hemin ($Fe^{3+}$), and hematin ($Fe^{3+}$) are all high spin compounds, the empirical correlation of reference 30 can be used to predict that the sign of $q$ in all three cases is positive. This result can be independently confirmed as discussed below.

The isomeric shift of Hb falls close to the normally observed range for high spin ferrous compounds. As discussed in the $Fe^{57}$ in Porphyrin Ring Compounds Section, the local symmetry immediately surrounding the Fe atoms in hemoglobin indicates that the EFG must be axially symmetric and directed perpendicular to the heme plane. Therefore, since the Zeeman selection rules indicate that transitions between the nuclear substates $+1/2 \rightarrow +3/2$ and $-1/2 \rightarrow -3/2$ will occur mainly along the EFG direction and the transitions $\pm 1/2 \rightarrow \pm 1/2$ mainly perpendicular to the EFG, the weaker intensity line in Fig. 3*d* and *e* is associated with transitions to the $I_z = \pm 3/2$ excited nuclear state in the Hb molecule. Using the known positive sign of the $Fe^{57}$ 14.4 kev excited state quadrupole moment, equation (7) indicates that $q$ in Hb must be positive ($V_{zz}$ is negative).

The iron atoms in hemin and hematin are in the $Fe^{3+}$ high spin state. The $d$ electrons in these atoms have parallel spins with a spin quantum number $S = 5/2$. Mössbauer spectra of hemin at various temperatures have been obtained by several groups (7, 31–38), but the data are in poor agreement and the interpretation of these spectra seems not well understood. At 5°K a quadrupole split spectrum (peak separation 0.78 mm/second) with lines of equal intensity was found (Fig. 3*g*). Similar spectra have been reported by Shulman and Wertheim (36) and recently by Bearden *et al.* (38). The low temperature spectrum of hematin (Fig. 3*h*) is similar with a somewhat larger quadrupole splitting (peak separation 0.98 mm/second).

The isomeric shift of hemin and hematin falls within the region of other high spin $Fe^{3+}$ compounds. Between liquid helium and liquid nitrogen temperature, the spectra of hemin and hematin change considerably. The high velocity line is drastically broadened, although the absorption area under the two lines remains roughly equal to within experimental error. The effect, therefore, cannot be attributed to a directional dependence of $f$ as is observed in Hb. We feel that this effect is probably caused by a long spin lattice relaxation time (on the order of the nuclear Larmor precessional frequency) of atoms in the $S_z = \pm 3/2$ and $\pm 5/2$ states which become populated at higher temperatures. The line broadening is then due to a magnetic hyperfine interaction (since the time average of the internal magnetic field is no longer zero) which initially splits the $I_z = \pm 3/2$ excited nuclear state three times faster than the $I_z = \pm 1/2$ excited state. A similar effect has been observed in corundum (39) and has been theoretically postulated by Blume (40). If this interpretation is correct, equation (7) again indicates that $q$ is positive in agreement with our above conclusion.

The sign of the EFG cannot be determined from the spectra of $O_2$-Hb and CO-Hb, and the quadrupole split lines appear to have the same intensity at all temperatures to within experimental error. The isomeric shifts of these spectra fall about 0.1 mm/second higher in velocity than the range [$-0.5 \rightarrow -0.2$ mm/second] normally observed in both low spin $Fe^{II}$ and $Fe^{III}$ compounds. A general correlation between $\delta$ and $\Delta E_Q$ is not well established in low spin ferrous and ferric compounds (possibly because a large abundance of data is not as yet available). Within our experimental accuracy $\delta$ for both $O_2$-Hb and CO-Hb is the same, although there is a large difference in $\Delta E_Q$. The sign of the EFG at the Fe nuclei in these molecules could be determined with the use of a large external magnetic field to observe a magnetic hyperfine splitting in these molecules. The possibility that Fe in $O_2$-Hb could be in the $Fe^{III}$ state (rather than the normally accepted $Fe^{II}$ state) has been proposed recently (41). It is unfortunate that the isomeric shift of the Mössbauer spectrum does not allow one to make a clear cut distinction in this case; however, because the quadrupole splitting observed in $O_2$-Hb is considerably larger than is normally observed in $Fe^{III}$ compounds, we feel it is somewhat more likely that the iron in $O_2$-Hb is in the ferrous state. In ionic compounds the difference between $Fe^{2+}$ and $Fe^{3+}$ is obvious; however, in low spin iron compounds the distinction depends on assigning covalently bonded electrons to specific atoms and in this case the difference between $Fe^{II}$ and $Fe^{III}$ may not be particularly meaningful.

*The EFG in Hemoglobin.* The bonding to the Fe atoms in hemoglobin must be essentially ionic since this is a "high spin" compound with a measured effective magnetic moment of 5.46 Bohr magnetons per heme (42). Hund's rule for the $Fe^{2+}$ ion predicts a $^5D$, $3d^6$ ground state for this ion (a half-filled $d$ shell with parallel spins plus one $d$ electron of opposite spin) and assuming the orbital

angular momentum is completely quenched, an effective magnetic moment of $[S(S + 1)]^{\frac{1}{2}} = 4.90$ Bohr magnetons is predicted, in reasonable agreement with experiment. We can, therefore, treat the $Fe^{2+}$ in hemoglobin as being purely ionic and consider the electric field gradient as resulting from the odd *d* electron (the half-filled *d* shell is spherically symmetric and produces no electric field gradient). The degeneracy of the five atomic *d* orbitals is removed by the crystalline (or molecular) electric field as shown schematically in Fig. 8. A direct interaction of the crystalline

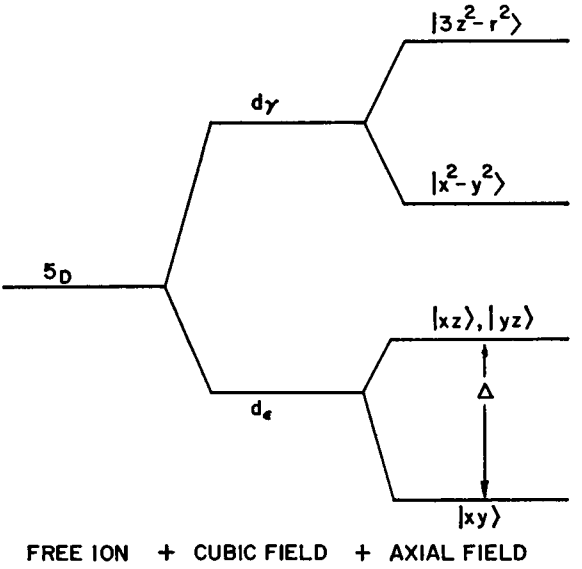


FIGURE 8 Splitting of the ferrous ion energy levels by the crystalline (or molecular) field.

field with the nucleus is much smaller than the interaction due to the odd *d* electron and for our purposes this effect will be neglected.

The positive sign of $q$ in hemoglobin (Discussion section) establishes that the lowest lying *d* orbital is either $|xy\rangle$ or $|x^2-y^2\rangle$ (17). A crystalline field with cubic symmetry splits the *d* orbitals into 2 groups, the triplet $d_\epsilon$ group and the doublet $d_\gamma$ group (43). Since the N atoms surrounding the Fe atoms in hemoglobin possess a negative charge, the triplet state, whose wave functions do not point toward these atoms, will lie lowest in energy (this splitting in $Fe^{2+}$ compounds is typically about $10^4$ $cm^{-1}$). The $|xy\rangle$ orbital is the only member of $d_\epsilon$ which produces a positive $q$, and therefore, this wave function must be the ground state in hemoglobin.

Because the central structure of the hemoglobin molecule immediately surrounding the $Fe^{2+}$ ions has an approximate fourfold rotation axis, we have assumed an axially symmetric electric field gradient which has the effect of splitting the $d_\epsilon$ triplet into two energy levels: a singlet ground state $|xy\rangle$ and a doubly degenerate state $|xz\rangle$

and $|yz\rangle$ at an energy $\Delta$ above the ground state. If the nuclear relaxation time is long compared with the transition times between the $d$ orbitals (44) and we ignore the effects of spin-orbit coupling, we can then estimate $\Delta$ from the temperature dependence of $\Delta E_Q$ by averaging the contributions to the electric field gradient from the $d_\epsilon$ levels weighted by an appropriate Boltzmann factor

$$q = \frac{\sum_n q_n e^{-\Delta_n/kT}}{\sum_n e^{-\Delta_n/kT}} \tag{23}$$

and noting that the electric field gradient produced by an electron in the $|xz\rangle$ and $|yz\rangle$ orbitals is $\frac{1}{2}$ that produced by an electron in the $|xy\rangle$ orbital and of the opposite sign. We have assumed that the $d_\gamma$ orbitals lie high enough in energy so that their contribution to the electric field gradient is negligible, but low enough in energy so that the $d$ shell remains half filled. The symbol $q_n$ in equation (23) represents the value of $q$ produced by an electron in the $n^{th}$ orbital and $\Delta_n$ is the energy separation of the $n^{th}$ orbital from the ground state. The low temperature quadrupole splitting (peak separation = 2.36 mm/second at 5°K) is then proportional to the shielded electric field gradient produced by an electron in the $|xy\rangle$ orbital and $\Delta \simeq 420$ cm$^{-1}$ ($\Delta/k \simeq 600$°K). The theoretical curve based on this value $\Delta$ is shown as a solid line in Fig. 7. The values of $\Delta$ observed in various $Fe^{2+}$ compounds are typically on the order of $10^2$ to $10^3$ cm$^{-1}$ (17) which makes the value observed in hemoglobin seem reasonable; however, in view of the assumptions made, this number should be regarded as a rough estimate.

The authors gratefully acknowledge many helpful discussions with Dr. A. H. Muir, Jr., Dr. H. Wiedersich, Dr. L. E. Topol, and Dr. W. J. Frajola, and the technical assistance of M. R. Bloombaum, A. C. Micheletti, and K. G. Rasmussen.

*Received for publication, May 24, 1965.*

## REFERENCES

1. Proceedings of the First Conference of the Mössbauer Effect, Urbana, University of Illinois, (H. Frauenfelder and H. Lustig, editors), 1960.
2. Proceedings of the Second International Conference of the Mössbauer Effect, 1961, Saclay, France, (D. M. J. Compton and A. H. Schoen, editors), New York, John Wiley & Sons, Inc., 1962.
3. Proceedings of the Third International Conference of the Mössbauer Effect, 1963, Ithaca, New York, Cornell University, (A. J. Bearden, editor), *Rev. Mod. Phys.*, 1964, **36**, 333.
4. MUIR, A. H., and ANDO, K. J., The Mössbauer Effect Data Index, Thousand Oaks, California, North American Aviation Science Center, 1964.
5. MÖSSBAUER, R. L., *Z. Physik.*, 1958, **151**, 124.
6. MÖSSBAUER, R. L., *Naturwissenschaften*, 1958, **45**, 538.
7. GONSER, U., and GRANT, R. W., Symp. Mössbauer Effect Methodology, New York, Plenum Press, 1965.
8. BOYLE, A. J. F., and HALL, H. E., *Rep. Progr. Phys.*, 1962, **25**, 441.
9. FRAUENFELDER, H., The Mössbauer Effect, New York, W. A. Benjamin, Inc., 1962.

10. GOL'DANSKII, V. I., The Mössbauer Effect and Its Applications in Chemistry, Moscow, Academy of Sciences Press, 1963.
11. WERTHEIM, G. K., Mössbauer Effect. Principles and Applications, New York, Academic Press, Inc., 1964.
12. MÖSSBAUER, R. L., and WIEDEMANN, W. H., *Z. Physik.* 1960, **159,** 33.
13. MUIR, A. H., Atomics International Report #6699, 1962.
14. SHIRLEY, D. A., *Rev. Mod. Phys.,* 1964, **36,** 339.
15. GEORGE, P., BEETLESTONE, J., and GRIFFITH, J. S., *Rev. Mod. Phys.,* 1964, **36,** 441.
16. KENDREW, J. C., *Science,* 1963, **139,** 1259.
17. INGALLS, R., *Physic. Rev.,* 1964, **133,** 787.
18. GONSER, U., GRANT, R. W., and KREGZDE, J., *Science,* 1964, **143,** 680.
19. MARGULIES, S., and EHRMAN, J. R., *Nuclear Instr. and Methods,* 1961, **12,** 131.
20. NUSSBAUM, R. H., and HOUSLEY, R. M., to be published.
21. SHIRLEY, D. A., KAPLAN, M., and AXEL, P., *Physic. Rev.,* 1961, **123,** 816.
22. GOL'DANSKII, V. I., MAKAROV, E. F., and KHRAPOV, V. V., *Physical Rev. Letters,* 1963, **3,** 344.
23. FLINN, P. A., RUBY, S. L., and KEHL, W. L., *Science,* 1964, **143,** 1434.
24. TOWNES, C. H., and SCHAWLOW, A. L., Microwave Spectroscopy, New York, McGraw-Hill Book Company, 1955.
25. WALKER, L. R., WERTHEIM, G. K., and JACCARINO, V., *Physic. Rev., Letters,* 1961, **6,** 98.
26. HERBER, R. H., KING, R. B., and WERTHEIM, G. K., *Inorg. Chem.* 1964, **3,** 101.
27. BARRETT, P. H., GRANT, *R.* W., KAPLAN, M., KELLER, D. A., and SHIRLEY, D. A., *J. Chem. Phys.,* 1963, **39,** 1035.
28. KERLER, W., NEUWIRTH, W., and FLUCK, E., *Z. Physik.,* 1963, **175,** 200.
29. COLLINS, R. L., and PETTIT, R., *J. Chem. Physics,* 1963, **39,** 3433.
30. REMY, P. H., and POLLAK, H., *J.. Appl. Physics,* 1965, **36,** 860.
31. REIZENSTEIN, P. G., and SWAN, J. B., International Biophysics Congress, 1961, 147.
32. GONSER, U., *Physic. Chem.,* 1962, **66,** 564.
33. EPSTEIN, L. M., *J. Chem. Physics,* 1962, **36,** 2731.
34. CRAIG, P. P., and SUTIN, N., *Phys. Rev. Letters,* 1963, **11,** 460.
35. MALING, J. E., and WEISSBLUTH, M., *in* Electronic Aspects of Biochemistry, (B. Pullman, editor), New York, Academic Press, Inc., 1964, 93.
36. SHULMAN, R. G., and WERTHEIM, G. K., *Rev. Mod. Physics,* 1964, **36,** 457.
37. KARGER, W., Berichte der Bunsengesellschaft, 1964, **68,** 793.
38. BEARDEN, A. J., MOSS, T. H., CAUGHEY, W. S., and BEAUDREAU, C. A., to be published.
39. WERTHEIM, G. K., and REMEIKA, J. P., *Physic. Rev. Letters,* 1964, **10,** 14.
40. BLUME, M., *Physic. Rev. Letters,* 1965, **14,** 96.
41. WEISS, J. J., *Nature,* 1964, **202,** 83.
42. PAULING, L., and CORYELL, C. D., *Proc. Nat. Acad. Sc.,* 1936, **22,** 210.
43. BLEANEY, B., and STEVENS, K. W. H., *Rep. Progr. Physics,* 1963, **16,** 108.
44. LANG, L. G., DEBENEDETTI, S., and INGALLS, R. L., *J. Physic. Soc., Japan,* 1962, **17,** suppl. B-1 131.